

Birefringence in ordered Ga_{0.47}In_{0.53}As/InP

R. Wirth, J. Porsche, F. Scholz, and A. Hangleiter

4. Physikalisches Institut, Universität Stuttgart, Pfaffenwaldring 57, D-70550 Stuttgart, Germany

(Received 21 July 1998)

The ordering-induced birefringence in spontaneously ordered Ga_{0.47}In_{0.53}As grown on InP substrates is studied. For this purpose, a photoelastic modulator was used, allowing a direct measurement of the birefringence in a spectral range between 0.67 and 1.0 eV. Near the band gap the birefringence peaks up to $\Delta n = n_e - n_o = -0.03$. By comparison of Kramers-Kronig transformed data of the dichroism to the measured birefringence, we show that the dispersion of birefringence may be understood by the valence-band splitting and the anisotropic optical matrix element. However, there is an offset between the birefringence data deduced from dichroism and the directly measured birefringence. This offset probably is caused by the anisotropy of the E_1 and $E_1 + \Delta_1$ critical points as confirmed by reflectance difference spectroscopy. [S0163-1829(99)01503-9]

Spontaneous chemical ordering in ternary III-V semiconductor alloys leads to a reduction of the crystal symmetry. In the case of CuPt_B-type ordering the tetrahedral symmetry T_d of the zinc-blende structure is reduced to C_{3v} . This leads to an uniaxial dielectric tensor with the extraordinary axis aligned to the ordering direction $[1\bar{1}1]$.¹ Although it is evident that a CuPt_B-type-ordered crystal has to be birefringent, taking into account the ordering-induced valence-band splitting and the anisotropic optical matrix element at the band gap,² the ordering-induced birefringence has been observed only recently for ordered Ga_{0.51}In_{0.49}P.^{3,4} These measurements show a positive birefringence $\Delta n = n_e - n_o$ far below the band gap and a negative birefringence up to $\Delta n = -0.02$ when approaching the band gap. However, the experimental methods that have been used, i.e., the analysis of the modified mode structure in an ordered waveguide³ and the polarization-dependent measurement of Fabry-Pérot interferences,⁴ fail above the fundamental band gap due to absorption.

We used a photoelastic modulator⁵ (PEM) to measure the ordering-induced birefringence of Ga_{0.47}In_{0.53}As grown lattice matched to InP. A PEM produces a sinusoidally modulated phase shift $A\sin(\omega t)$ between the two components of the incident light polarized along its principal axes at a fixed angular frequency ω . The polarization modulated light emerging from a PEM in connection with lock-in technique may be used to measure very small effects of birefringence. The high sensitivity of this modulation technique to small birefringence-induced phase shifts allow measurements well down to $\Delta nkL = 0.001$, where k is the wave vector and L is the samples thickness. Thus, if thin samples in the range between 1 and 2 μm are used, measurements of birefringence even above the band gap may be carried out.

Our experimental setup is shown in Fig. 1. For the birefringence measurement in the infrared region a tungsten halide lamp and for the reflectance difference spectroscopy up to 5.5 eV a xenon arc lamp has been used. The light was sent through a 1-m grating monochromator. The spectral resolution in the experiments presented in this paper was better than 2 nm in all cases. The PEM's fixed modulation frequency was $\omega = 84$ kHz. For detection high-speed Ge and Si diodes in connection with an amplifier (transimpedance $\approx 5 \times 10^6$ V/A) have been used. The bandwidth of the photodiode/amplifier unit was >1 MHz.

Using Jones matrices for the optical components it may be shown easily that the intensity of the probe light shows the following modulation behavior:

$$I \sim \cosh(\Delta \kappa k L) - \cos[\Delta n k L + A \sin(\omega t)], \quad (1)$$

where $\Delta \kappa$ is the difference in the extinction coefficients of the sample for polarization along the principal axes of the modulator, hence describing the samples dichroism. Δn is the birefringence of the sample. Expanding the last term of Eq. (1) into a Fourier series up to the first order leads to

$$I \sim \cosh(\Delta \kappa k L) - J_0(A) \cos(\Delta n k L) - 2J_1(A) \sin(\Delta n k L) \sin(\omega t) \quad (2)$$

where J denotes the Bessel function.

The dc component of this modulated intensity may be made independent of the samples birefringence Δn , if the retardation is chosen such that $J_0(A_0) = 0$, i.e., $A_0 \approx 2.405$. If we define the ratio $r = V_{\omega}^{\text{RMS}}/V_{\text{dc}}$ of the lock-in voltage obtained from the component oscillating at ω and the dc component of the detectors voltage, we find

$$\sin(\Delta n k L) = \frac{\cosh(\Delta \kappa k L)}{\sqrt{2} J_1(A_0)} r. \quad (3)$$

Since it is known that the dichroism in ordered materials peaks near the band gap due to the ordering-induced valence-band splitting,² the absorption at the band gap may be taken

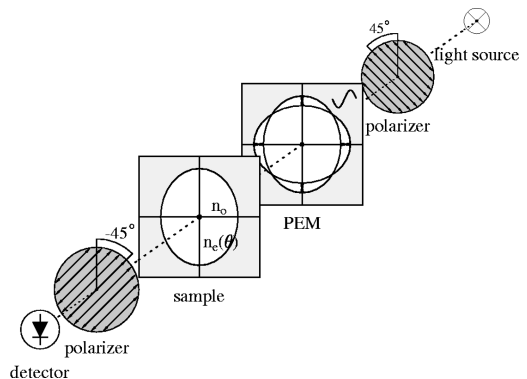


FIG. 1. Experimental setup for the measurement of the ordering-induced birefringence.

as an upper limit for the dichroism. For $\text{Ga}_x\text{In}_{1-x}\text{As}$ this is about $\alpha \approx 8000 \text{ cm}^{-1}$ or $\kappa \approx 0.1$. Because of this replacing $\cosh(\Delta\kappa kL)$ by 1 in Eq. (3) leads to a maximum error of 0.5%.

Also due to the birefringence the peak energies of Fabry-Pérot resonances are shifted with respect to each other for different polarizations⁴ leading to different transmission coefficients. However, a more complex calculation than the one presented above shows that even under worst case conditions, i.e., pronounced Fabry-Pérot resonances as a single $\text{Ga}_{0.47}\text{In}_{0.53}\text{As}$ layer surrounded by air would show, the effect on our experimental results is below 5% and should be smaller under realistic conditions.

To correct for residual birefringence and dichroism of the experimental setup a second measurement with the sample rotated by 90° has been taken. This switches the sign of the measured birefringence that emerges from the sample. Calculating the birefringence using Eq. (3) and subtracting both measurements removes the residual birefringence of the experimental setup. Above 1.1 eV the signal becomes small due to absorption. A small drift of the detectors dc offset between the two measurements will lead to wrong values of birefringence. However below 1.0 eV the measured birefringence is reproducible very well. Also the birefringence of the substrate without any $\text{Ga}_{0.47}\text{In}_{0.53}\text{As}$ layer has been measured and found to be negligible. All measurements in this paper have been performed at room temperature.

We used samples with single $1\text{-}2\text{-}\mu\text{m}$ -thick $\text{Ga}_{0.47}\text{In}_{0.53}\text{As}$ layers grown by low pressure metal organic vapor-phase epitaxy at a growth temperature of 560°C and a V/III ratio of 30. The layers have been grown lattice matched on InP substrates with the (001) surface tilted by $2^\circ\text{-}15^\circ$ towards one of the nearest $\{111\}_B$ planes. Similar to $\text{Ga}_x\text{In}_{1-x}\text{P}$, the tilt of the substrate towards $\{111\}_B$ leads to single-variant ordering in $\text{Ga}_{0.47}\text{In}_{0.53}\text{As}$.⁶ The strength of ordering in this series of samples varies from weakly ordered samples on the strongly tilted substrates to samples that show rather strong ordering on the 2° off substrate.⁷ The strength of ordering usually is described by the ordering parameter $\eta = |p_{\text{Ga}} - p_{\text{In}}| / (p_{\text{Ga}} + p_{\text{In}})$, where p_{Ga} and p_{In} are the probabilities to find a Ga or a In atom in one of the $\{111\}_B$ -ordering planes, respectively.

The measured birefringence scales with the degree of ordering, as well as with the inhomogeneous broadening, that is seen in absorption measurements. However, qualitatively the experimental data is similar for all ordered samples. Therefore, we will focus in the following on a sample grown on a 6° off substrate showing the least-broadened absorption spectrum. The sample thickness was $1.6 \mu\text{m}$. Using x-ray diffraction we found almost perfect lattice matching, with a slight tensile strain of about 0.03%. Also the x-ray line width is comparable to disordered reference samples. The valence-band splitting and band-gap reduction of this sample has been determined previously⁷ to be 12 and 29 meV, respectively. Using the recently published value for the crystal-field splitting of perfectly ordered $\text{Ga}_{0.47}\text{In}_{0.53}\text{As}$,⁸ i.e., $\Delta_{CF} = 0.13 \text{ eV}$, a degree of ordering of $\eta = 0.38$ may be assigned to this sample. As a disordered reference we used a $4.0\text{-}\mu\text{m}$ -thick $\text{Ga}_{0.47}\text{In}_{0.53}\text{As}$ sample grown by liquid-phase epitaxy (LPE) on an exactly oriented (001) InP substrate.

In CuPt_B -type single-variant-ordered samples the dielec-

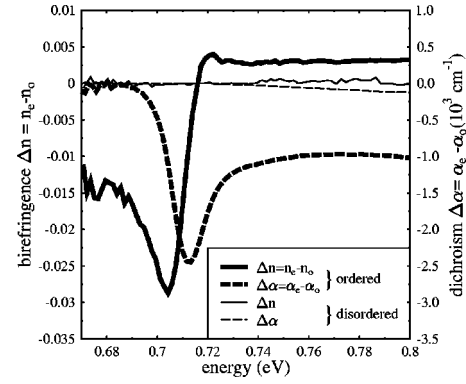


FIG. 2. Birefringence and dichroism for ordered and disordered $\text{Ga}_{0.47}\text{In}_{0.53}\text{As}/\text{InP}$.

tric tensor is uniaxial and the extraordinary axis is aligned parallel to the ordering direction, which we choose here to be the $[1\bar{1}1]$ direction. The angle between $[001]$ and $[1\bar{1}1]$ is 54.74° and the extraordinary axis in our sample is $\theta = 54.74^\circ - 6^\circ$ with respect to the sample's surface considering the tilt of the substrate. If the sample's $[110]$ and $[1\bar{1}0]^*$ directions (where $*$ denotes deviation to the exact $[1\bar{1}0]$ direction due to the tilt of the substrate) are aligned parallel to the principal axes of the modulator, the birefringence $\Delta n(\theta) = n_{[1\bar{1}0]^*} - n_{[110]} = n_e(\theta) - n_o$ is measured. To derive the birefringence of the uniaxial tensor $\Delta n = n_e - n_o$ the equation for the indicatrix

$$\frac{1}{n(\theta)^2} = \frac{\sin^2(\theta)}{n_e^2} + \frac{\cos^2(\theta)}{n_o^2} \quad (4)$$

may be used. After replacing $n_e = n_o + \Delta n$ and $n_e(\theta) = n_o + \Delta n(\theta)$ Eq. (4) may be solved for $\Delta n = \Delta n[n_o, \Delta n(\theta)]$. Fortunately $\Delta n[n_o, \Delta n(\theta)]$ is independent of n_o in the first-order term. For $\theta = 54.47^\circ - 6^\circ$ we find

$$\Delta n = \frac{1}{\sin^2(\theta)} \Delta n(\theta) \approx 1.77 \times \Delta n(\theta), \quad (5)$$

with an error below 0.2% for the Taylor expansion.

Besides the birefringence, we also measured the absorption for light polarized along $[110]$ and $[1\bar{1}0]^*$ using a standard absorption setup. The absorption data may be transformed in a similar way as described above into $\Delta\alpha = \alpha_e - \alpha_o$, which describes the dichroism of the sample.

In Fig. 2 the measured birefringence and the dichroism for the ordered sample as well as for the disordered reference sample are shown from 0.67 eV up to 0.8 eV. The room-temperature band gaps of the ordered and disordered samples are 0.71 and 0.74 eV, respectively. The LPE-grown sample shows almost no birefringence and very weak dichroism, which probably reflect stability problems of the dichroism measurement, which has been performed without using a modulation technique, and not real-sample features. On the other hand the ordered sample shows a strong dichroism at the band gap due to the valence-band splitting and anisotropic interband matrix element. Between the conduction band and the topmost valence band only transitions polarized parallel to the ordering planes are allowed,⁹ making contributions to α_o , whereas transitions to the second valence band are allowed for all polarizations with a preference for

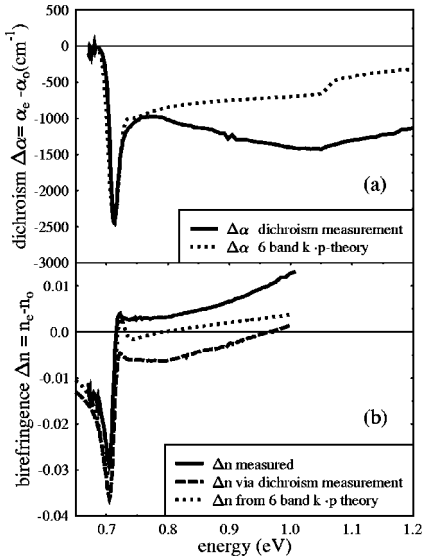


FIG. 3. (a) measured and calculated dichroism of ordered $\text{Ga}_{0.47}\text{In}_{0.53}\text{As}$. Calculation due to six-band $\mathbf{k}\cdot\mathbf{p}$ theory. (b) Comparison of directly measured birefringence, birefringence deduced from dichroism measurements and six-band $\mathbf{k}\cdot\mathbf{p}$ calculations.

polarization along the ordering direction $[1\bar{1}1]$, therefore making stronger contributions to α_e . Thus, the dichroism peaks between the first and second valence band at about 2500 cm^{-1} , where this peak value varies strongly with the broadening for different ordered samples. At $\approx 1.0\text{ eV}$ [see Fig. 3(a)] the dichroism shows a strongly broadened kink and reduces further. This is due to transitions to the split off band. The birefringence of the ordered sample starts with negative values below the band gap and peaks at the band gap with a value of $\Delta n = -0.03$. Above the band gap we find a birefringence of $\Delta n = 0.003$. The peak value of $\Delta n = -0.03$ is larger than the values that have been reported for $\text{Ga}_{0.47}\text{In}_{0.53}\text{As}$.^{3,4} However, both experimental methods used in the previous work on birefringence of ordered samples fail as absorption becomes strong at the band gap, and hence they have not been able to measure up to energies where the birefringence has its peak value.

When performing a Kramers-Kronig (KK) transformation of our experimental dichroism data between 0.67 eV and 1.2 eV the shape of the birefringence is perfectly reproduced [see Fig. 3(b)]. However, the birefringence spectrum deduced from dichroism data is shifted by about 0.01 towards negative values compared to the actual birefringence. Since this shift is practically constant over the range between the band gap and 1.0 eV it cannot emerge from any features near the band gap. Rather this is indicating that this shift is the ‘‘foothill’’ of an anisotropic oscillator far away from the band gap. Actually the shift of the birefringence has been observed also for ordered $\text{Ga}_{0.51}\text{In}_{0.49}\text{P}$, where the birefringence far below the band gap again becomes positive.^{3,4} We expect a similar crossover to positive birefringence far below the band gap for $\text{Ga}_{0.47}\text{In}_{0.53}\text{As}$. However, this isotropic point would be found around 0.5 eV, outside the spectral range of our experimental setup.

To understand the reason for the shift between the actual birefringence and the birefringence deduced from the dichroism measurement, we calculated the dichroism using a six-band $\mathbf{k}\cdot\mathbf{p}$ theory. A Hamiltonian for ordered bulk materials

proposed by Wei and Zunger¹⁰ was used, discrete excitons, and excitonic enhancement were included. The dichroism $\Delta\alpha$ was calculated by \mathbf{k} -space sampling, hence including the important \mathbf{k} dependence of the interband matrix element, which cannot be neglected.¹¹ The dichroism was calculated between the band edge and 1.2 eV and converted to birefringence data by KK transform (see Fig. 3). Up to $\approx 30\text{ meV}$ above the band gap the calculated and measured dichroism is in good agreement. However, going to higher photon energies the $\mathbf{k}\cdot\mathbf{p}$ theory underestimates the dichroism. Thus the birefringence deduced from this calculation is in reasonable agreement below the band gap [see Fig. 3(b)]. Also the calculation reproduces the transition of the birefringence to positive values where the dichroism has its peak value. This positive birefringence above the band gap has been predicted by Zhang and co-workers⁴ using an eight-band $\mathbf{k}\cdot\mathbf{p}$ calculation. However, this correct prediction from $\mathbf{k}\cdot\mathbf{p}$ calculations is an artifact due to the underestimation of the dichroism above the band gap, since birefringence data derived from the dichroism measurement within the same energy range show no positive birefringence near the band gap [see Fig. 3(b)]. Above the band gap neither the form of the birefringence spectrum, nor the values are reproduced by $\mathbf{k}\cdot\mathbf{p}$ calculations. The reason for the underestimation of the dichroism probably are the nonparabolicities of the conduction band. In our model we used a simple symmetric parabolic conduction band, even in the eight-band $\mathbf{k}\cdot\mathbf{p}$ calculations of Zhang and Mascarenhas¹¹ the conduction band is only dependent quadratically on k . On the other hand, it is well known, that the conduction band in $\text{Ga}_{0.47}\text{In}_{0.53}\text{As}$ shows a strong nonparabolicity. This nonparabolicity has been measured by photoconductivity¹² up to 40 meV above the conduction-band edge and may be described using a fourth order term in \mathbf{k} (see Ref. 13),

$$E_c = E_0 - E_0^2 \left(1 - \frac{m_0^*}{m_0} \right)^2 \left(\frac{1 + x + \frac{1}{4}x^2}{1 + \frac{4}{3}x + \frac{4}{9}x^2} \right) \frac{1}{E_G}, \quad (6)$$

where x is the ratio of band-gap energy to spin-orbit splitting energy, m_0^* is the conduction-band mass, and $E_0 = (\hbar^2 k^2)/(2m_0^*)$. Unfortunately this formula is only valid in the same energy range where the photoconductivity data are available and becomes nonphysical beyond 8% of the Brillouin zone. However, if we use this formula for the nonparabolic conduction band in our calculations up to about 40 meV above the band gap we find a good agreement of the slope of measured and calculated absorption spectra, whereas the slope above the band gap is underestimated if a parabolic conduction band is used. Thus we conclude that quantitative calculations of absorption, dichroism, and birefringence near the band gap have to include the nonparabolicity of the conduction band. On the other hand, if one succeeds including the nonparabolicity up to about 1.2 eV this probably will result in birefringence data similar to the data we derived from KK transformed dichroism measurements, reproducing the form of the measured birefringence but shifted to negative values [see Fig. 3(b)]. So, since the shift and the positive birefringence far below the band gap cannot be understood due to the anisotropic interband matrix elements at the band gap, we looked for other anisotropic contributions to the di-

electric function far above the band gap using reflectance difference spectroscopy (RDS).

Several RDS investigations have been performed for ordered $\text{Ga}_{0.51}\text{In}_{0.49}\text{P}$ by Luo and co-workers.^{14–16} We used a similar experimental setup, to achieve high sensitivity for the difference of the reflection $\Delta R/R = 2(R_{[1\bar{1}0]^*} - R_{[110]}) / (R_{[1\bar{1}0]^*} + R_{[110]})$ for polarization along $[110]$ and $[1\bar{1}0]^*$. As shown above the birefringence setup (Fig. 1) is rather insensitive to dichroism or differences in the transmitted light for the two polarizations. On the other hand, the RDS setup measures the differences of the reflected light for different polarization and thus is strongly affected by Fabry-Pérot resonances that appear together with birefringence so that the peak positions of the resonances for different polarization are shifted slightly with respect to each other.⁴ Because of this our RDS measurements show strong peaking below 1.2 eV actually shadowing the near band-gap RDS features that Luo and co-workers have observed.¹⁶ To overcome this problem they used thick samples, where the resonances are damped by absorption. However, we would like to focus on the RDS spectra above 1.2 eV, since our dichroism measurements show no pronounced anisotropic features between 0.8–1.2 eV that could lead to the shifted birefringence at and below the band gap.

Taking into account that above ≈ 2 eV the penetration depth of the light is only a few monolayers, it is difficult to extract quantitative information about the bulk material anisotropy from RDS measurements. Although it is known that pronounced RDS features due to surface reconstruction are quenched when samples are exposed to air,¹⁵ even the disordered LPE grown sample shows a ramp like RDS signal between 1 and 3 eV, that disappears above 4 eV in Fig. 4. The RDS spectrum of the ordered sample shows strong peaks at E_1 and $E_1 + \Delta_1$, which may be found at ≈ 2.6 eV and ≈ 2.8 eV, respectively.¹⁷ Similar to the disordered sample the RDS signal fades away above 4 eV. So, although the ordering induced anisotropy of the bulk crystal mingles with surface effects, we conclude from our RDS measurements that the anisotropy at the E_1 critical point influences the birefringence even at the band gap, whereas the E_0, E_2 , and $E_2 + \Delta_2$ critical points between 4.4–5.2 eV do not seem to result in strong anisotropic absorption, making no or only weak contributions to the birefringence. It is interesting to

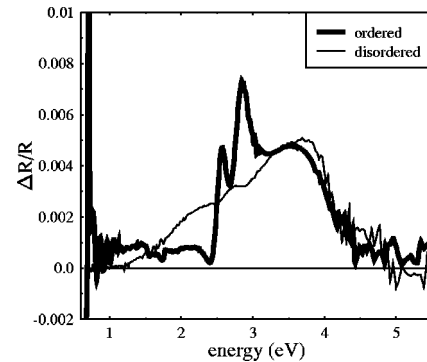


FIG. 4. Reflectance difference spectra of ordered and disordered $\text{Ga}_x\text{In}_{1-x}\text{As}$, where $\Delta R/R$ is defined as $2(R_{[1\bar{1}0]^*} - R_{[110]}) / (R_{[1\bar{1}0]^*} + R_{[110]})$.

note the similarities to the piezo-birefringence of zincblende crystals for stress along $[111]$, where the stress mainly affects states near the L point of the Brillouin-zone, whereas states near the X point make no contribution to birefringence in the first order.¹⁸ The contribution of the E_1 critical point there establishes the isotropical point of the piezobirefringence below the band gap, that is common to almost all zinc-blende crystals.

Since experimental methods to measure the optical anisotropy in the spectral range of E_1 and E_2 are all based on reflection (i.e., RDS or ellipsometry), all these methods suffer from surface effects measuring the so-called “pseudodielectric” function. However, theoretical calculations of the dielectric function of ordered crystals may be compared to birefringence measurements. Up to now ordering-induced level splittings at E_1 and E_2 have been predicted¹⁹ and observed,^{1,20} but no quantitative calculations of the anisotropies near E_1 and E_2 have been performed.

In conclusion, we have measured the ordering-induced birefringence of $\text{Ga}_{0.47}\text{In}_{0.53}\text{As}/\text{InP}$. The birefringence has its peak value of $\Delta n = -0.03$ at the band gap and becomes positive above band gap. $\mathbf{k} \cdot \mathbf{p}$ calculations near the band gap show that the nonparabolicity of the conduction band has to be included to reproduce the form of the birefringence spectrum. Also the optical anisotropy of the E_1 critical point, leading to an offset at the band gap, cannot be neglected when calculating the ordering-induced birefringence.

Financial support of this work by the Volkswagenstiftung is gratefully acknowledged.

¹F. Alsina *et al.*, in *Proceedings of the 22nd ICPS*, edited by D. J. Lockwood (World Scientific, Singapore, 1994), Vol. 1, p. 253.
²S. H. Wei and A. Zunger, *Phys. Rev. B* **49**, 14 337 (1994).
³R. Wirth *et al.*, *Phys. Rev. B* **55**, 1730 (1997).
⁴Y. Zhang *et al.*, *Solid State Commun.* **104**, 577 (1997).
⁵J. C. Kemp, *J. Opt. Soc. Am.* **59**, 950 (1969).
⁶R. Wirth *et al.*, *Appl. Phys. Lett.* **71**, 2127 (1997).
⁷R. Wirth *et al.*, *J. Appl. Phys.* **83**, 6196 (1998).
⁸S. H. Wei and A. Zunger, *Phys. Rev. B* **57**, 8983 (1998).
⁹A. Mascarenhas *et al.*, *Phys. Rev. Lett.* **63**, 2108 (1989).
¹⁰S. H. Wei and A. Zunger, *Appl. Phys. Lett.* **64**, 757 (1994).

¹¹Y. Zhang and A. Mascarenhas, *Phys. Rev. B* **51**, 13 162 (1995).
¹²R. J. Nicholas *et al.*, *J. Phys. C* **18**, L427 (1985).
¹³A. Raymond *et al.*, *J. Phys. C* **12**, 2289 (1979).
¹⁴J. S. Luo *et al.*, *J. Vac. Sci. Technol. B* **12**, 2552 (1994).
¹⁵J. S. Luo *et al.*, *J. Cryst. Growth* **174**, 558 (1997).
¹⁶J. S. Luo *et al.*, *Phys. Rev. B* **55**, 16 385 (1997).
¹⁷S. Adachi, *J. Appl. Phys.* **53**, 8775 (1982).
¹⁸A. Pikhtin and A. Yas'kov, *Fiz. Tekh. Poluprovodn.* **22**, 969 (1988) [*Sov. Phys. Semicond.* **22**, 613 (1988)].
¹⁹S. H. Wei, A. Franceschetti, and A. Zunger, *Phys. Rev. B* **51**, 13 097 (1995).
²⁰H. Lee *et al.*, *Phys. Rev. B* **53**, 4015 (1996).